Available online at www.sciencedirect.com
SCIENCE DIRECT®
Journal of Chromatography A, 1000 (2003) 779–800
JOURNAL OF CHROMATOGRAPHY A
www.elsevier.com/locate/chroma

Review

Determination of the interconversion energy barrier of enantiomers by separation methods

J. Krupcik[a,*], P. Oswald[a], P. Májek[a], P. Sandra[b], D.W. Armstrong[c]

[a]*Department of Analytical Chemistry, Slovak University of Technology, Radlinského 9, Bratislava 81237, Slovakia*
[b]*Department of Organic Chemistry, University of Ghent, Krijgslaan 281 S4, B-9000 Ghent, Belgium*
[c]*Department of Chemistry, Gilman Hall, Iowa State University, Ames, IA 50011-3111, USA*

Abstract

Separation methods have become versatile tools for the determination of kinetic activation parameters and energy barriers to interconversion of isomers and enantiomers in the last 20 years. New computer-aided evaluation systems allow the on-line determination of these data after separating minute amount of pure compounds or mixture of isomers or enantiomers, respectively. Both dynamic interconversion during the separation process as well as static stopped-flow techniques have been applied to determine the kinetic activation parameters and interconversion energy barriers by separation methods. The use of (1) combinations of batchwise kinetic studies with enantioselective separations, (2) a continuous flow model, (3) a comparison of real chromatograms with simulated ones, (4) stopped-flow techniques, (5) stochastic methods, (6) approximation functions and (7) deconvolution methods, for the determination of interconversion energy barriers by separation methods is summarized in detail.

Keywords: Reviews; Enantiomer separation; Energy barrier to interconversion; Interconversion energy barrier

Contents

*Corresponding author. Tel.: +421-7-532-5314; fax: +421-7-393-198.
E-mail address: krupcik@cvt.stuba.sk (J. Krupcik).

0021-9673/03/$ – see front matter
doi:10.1016/S0021-9673(03)00238-3

1. Introduction

It is well known that the biological activity of many drugs can be related to chirality. Frequently only one of the enantiomers shows the desired therapeutic effect while the other is inactive or shows undesirable effects. Since 1992, regulatory agencies have required extensive stereochemical information on chiral drugs [1]. Consequently, it is important to understand the conformational and/or configurational stability of those drugs that are administered as pure enantiomers. The process by which the individual enantiomers of chiral molecules undergo inversion of their respective stereogenic elements is referred to as enantiomerization [2]. The stability of enantiomers of thermally labile chiral drugs is thus naturally connected with an energy barrier to enantiomerization which can be determined by several methods. While the isolation of single enantiomers followed by an examination of batchwise racemization kinetics using chiroptical and NMR methods is cumbersome and time-consuming, enantioselective separation techniques tend to be more efficient since enantiomers are interconverted and analysed on-line, and they require only minute amounts of the racemic or enriched mixture of enantiomers [2–4].

Interconversion of conformationally or configurationally labile compounds have been investigated by means of dynamic NMR [5–7], chirooptical methods [4,8–13], dynamic gas chromatography (DGC) [4,14–48], dynamic supercritical fluid chromatography (DSFC) [4,49–51], dynamic high-performance liquid chromatography (DHPLC) [4,52–124], dynamic capillary electrophoresis (DCE) [4,125–129], dynamic micellar electrokinetic chromatography (DMEKC) [4,130–132] and dynamic capillary electrochromatography [4,133–138].

In enantioselective dynamic separation methods, interconversion processes are studied in the presence of a chiral stationary phase (CSP). Basically, seven experimental operational approaches have been exploited to determine rate constants and energy barriers by separation methods. They are:

(1) classical kinetic studies combined with enantioselective separations [136]

(2) methods based on the continuous flow model [56,127]

(3) comparison of real chromatograms with simulated ones (peak form analysis) [15,137,138]

(4) stopped-flow techniques [4,34,37,38,40,41,83],

(5) stochastic methods [4,66–69,142–144]

(6) approximation functions [139], and

(7) deconvolution methods [8,42,43].

The focus of this monograph is to provide an overview of the published works on the determination of kinetic parameters and energy barriers to interconversion of enantiomers of conformationally or configurationally labile compounds by enantioselective separation methods. A secondary aim is to describe a computer assisted peak deconvolution procedure for the determination of peak areas in peak clusters obtained by the separation of some 3-hydroxy-1,4-benzodiazepine drugs by DHPLC, DSFC and DMEKC. The corresponding peak areas were used to calculate rate constants and energy barriers to enantiomerization.

2. Theoretical

Two distinct systems can be used to study enantiomer interconversion.

2.1. Interconversion of enantiomers in static systems

The interconversion of enantiomers (*R* and *S*) in

static systems can be described as follows:

$$R \underset{k_{-1}}{\overset{k_1}{\rightleftarrows}} S$$

where k_1 and k_{-1} are the rate constants of the $R \rightarrow S$ and $S \rightarrow R$ interconversion, respectively. Interconversion of enantiomers in such systems is considered a reversible reaction and can be described by the first order kinetic equation. From the rate expression of reversible first-order reactions (assuming that the rate constants $k_1 = k_{-1} = k$ and no S enantiomer is present prior to interconversion) the following expression has been derived for the rate constant k [136,140]:

$$k = \frac{1}{2t} \ln \frac{c_{R0}}{2c_R - c_{R0}} \quad (1)$$

where c_{R0} is the initial concentration of enantiomer R and c_R is its concentration at time t.

The reversible interconversion of individual enantiomers in static systems leads to equilibrium with a constant, K [140]:

$$K = \frac{[R]}{[S]} = \frac{k_1}{k_{-1}} \quad (2)$$

where $[R]$ and $[S]$ are the equilibrium concentrations of enantiomers R and S, respectively.

If $k_1 = k_{-1}$, then the reversible interconversion of the enantiomers in a static system leads to a racemic mixture ($K = 1$) and this type of interconversion is known as racemization. Therefore, if enantiomers in a racemic mixture are reversibly interconverted in static systems, the equilibrium concentration of both enantiomers is constant ($[R] = [S]$), and independent of the time and temperature of interconversion.

2.2. Interconversion of enantiomers in dynamic systems

If the interconversion of enantiomers is not too fast and performed during a separation process, then the direct separation of a racemic or enriched mixture of thermolabile enantiomers can be considered as a reactive enantioselective separation. The enantiomerization rate, however, should allow the study of both the separation as well as the interconversion of enantiomers. Since chromatography and electromigration methods are dynamic systems where the original and the interconverted enantiomers are separated, the interconversions $R \rightarrow S$ and $S \rightarrow R$ may be considered as pseudo-irreversible [50] and can be described by an equation derived for the rate constant of irreversible first order reactions [140].

If the enantiomers are separated in an enantioselective system, the residence times of both enantiomers, $t_{R,S}$ and $t_{R,R}$, in this system differ and therefore the rate constants are supposed to be different:

$$k_1 = \frac{1}{t_{R,R}} \ln \frac{c_{R0}}{c_R} \quad (2a)$$

and

$$k_{-1} = \frac{1}{t_{R,S}} \ln \frac{c_{S0}}{c_S} \quad (2b)$$

where c is concentration, k is the rate constant and $t_{R,R}$ and $t_{R,S}$ are residence (retention) times of for the R and S enantiomers in the separation system, respectively [140].

3. Determination of the interconversion rate constants by separation methods

3.1. Combination of chiral separation with classical batchwise kinetic methods

In these methods, the interconversion of a pure enantiomer is performed outside of the separation system (off-line) at certain temperatures for the required time. Samples of the reaction mixture of enantiomers are then separated by enantioselective methods at temperatures where separation condition quenches the interconversion. Since achiral chromatographic detectors give equal responses for both enantiomers, the rate constants may be determined directly from peak areas obtained both by mass as well as for concentration types of detectors. However, the response of the latter type of detector depends on the mobile phase flow-rate. In chromatographic methods the mobile phase flow-rate is normally constant and the peak areas can be used directly in the calculation procedure. In capillary electrophoresis (CE) where the osmotic flow is not constant, the peak areas have to be corrected for

migration time prior their use in the calculation procedure. In classical kinetic studies the interconversion is performed in a stationary system, the forward rate constant is calculated from the modified Eq. (1):

$$k_1 = \frac{1}{2t} \ln \frac{c_{R,0}}{2c_R - c_{R,0}} = \frac{1}{2t} \ln \frac{A_{R,0}}{2A_R - A_{R,0}} \quad (3)$$

where t is the interconversion time, A is the peak area of the enantiomer R prior to ($A_{R,0}$), and after the interconversion (A_R). It is obvious that in CE methods corrected peak areas should be used. Fig. 1 shows chromatograms of the separation of a pure R-enantiomer (Fig. 1A), and after its partial (Fig. 1B and C) and final (Fig. 1D) interconversion (racemisation) in a static system.

If pure enantiomers are not accessible for kinetic study they can be produced on-line by enantioselective separation of a racemate at a low enough temperature. Separated enantiomers are then interconverted for a certain time at the desired temperature by stopping the mobile phase flow in the chiral or the achiral column [4,34,34,37,38,40,41,83]. Original and interconverted enantiomers are then separated on a chiral column. Thus, the applicability of this method requires that enantiomerization is suppressed during the chromatographic separation process. Such interconversion studies are known as stop-flow techniques.

3.2. Enantioselective stopped-flow methods

The stop-flow methods can be realized in a single chiral column or in a column series operated under multidimensional conditions [4,34,37,38,40,41,83, 101].

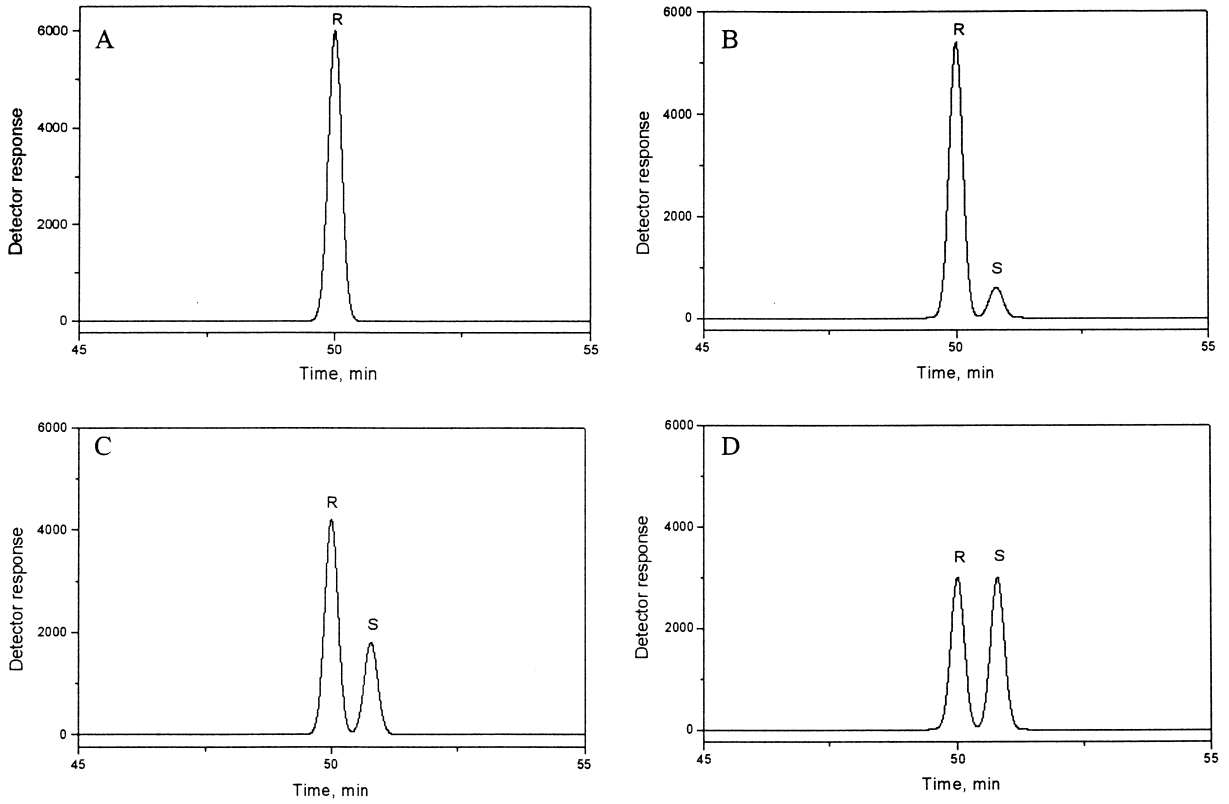

Fig. 1. Separation of R and S enantiomers by direct chiral chromatography at a temperature where interconversion of enantiomers is suppressed. (A) Pure enantiomer R; (B,C) partial interconversion of $R \rightarrow S$ enantiomer, D-racemic mixture.

3.2.1. Stopped-flow interconversion on single chiral column

As in dynamic methods, single-column stopped-flow techniques require the enantiomerization process to proceed in the environment of a liquid CSP, and the CSP is used to separate the enantiomers on-line. A single-column stopped-flow interconversion study is typically performed as follows. The enantiomers of the racemic mixture are quantitatively separated in the first part of the chiral column (CSP), the flow is stopped and the interconversion of the enantiomers is facilitated at an increased temperature by heating the entire column during an interconversion time. Subsequently, the original and interconverted enantiomers are separated in the second part of the column at the former separation temperature. It is obvious that the separation temperature (initial and final separation steps) has to be low enough so that the interconversion is suppressed during the separation process. The rate of conversion and the energy barrier to interconversion can be determined by variation of temperature and the interconversion time during which the flow of the mobile phase is stopped. In the presence of a chiral selector, the rates of interconversion may be different for both enantiomers, so that on the macroscopic level the ratio of *R* to *S* enantiomers deviates from the initial 50:50 ratio of the injected racemic mixture. This phenomenon is called deracemization [134].

Fig. 2 shows a four-peak pattern chromatogram obtained by the stopped-flow interconversion of enantiomers of a racemic mixture in a chiral column. The kinetic activation data and the enantiomerization barriers of both enantiomers are calculated from the corresponding peak areas (*A*), the enantiomerization time or (*t*), and the enantiomerization temperature (*T*).

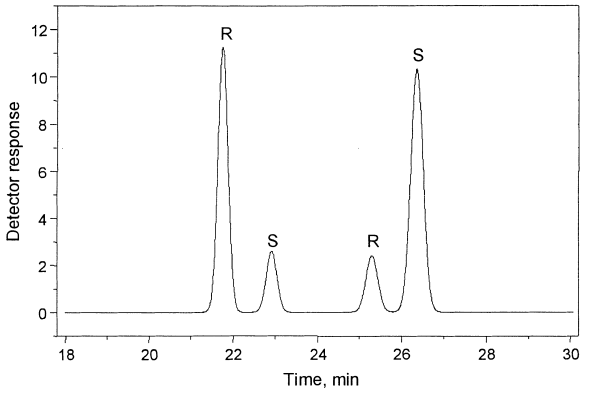

Fig. 2. Chromatogram obtained for the separation of enantiomers by the stopped-flow interconversion of enantiomers in racemic mixture in a chiral column.

As stated above, single on-column interconversion is accomplished in the presence of the chiral stationary phase. Accordingly, in comparison to free solution enantiomerization studies, more complex equilibria have to be considered, as illustrated in Fig. 3 [15,134].

On-column stop-flow interconversion in a single column was used for the determination of rate constants of enantiomers using stop-flow gas chromatography-sfHRGC [34,35,37,38,40,41], liquid chromatography-sfHPLC [101,102] and capillary electrokinetic chromatography–sf CEC [134].

3.2.2. Stop-flow interconversion in a column series operated under multidimensional conditions

The presence of the CSP in the single-column stop flow method can affect the interconversion rates. The barrier may be enhanced [21,101,116] or depressed [118]. Efforts have been made to combine the advantages of the stopped-flow approach with the option to perform enantiomerization in an achiral and

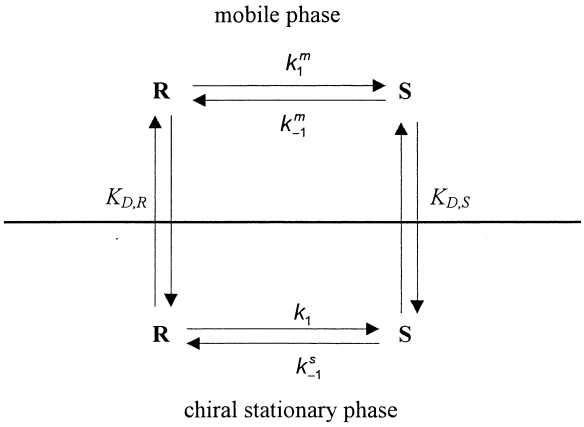

Fig. 3. Schematic of the processes occurs during on-column interconversion [15]. $K_{D,R}$ and $K_{D,S}$ are the partition constants of *R* and *S* enantiomers between mobile and stationary phases, k_1^m and k_{-1}^m are rate constants of the $R \rightarrow S$ and $S \rightarrow R$ interconversion in the mobile phase, respectively k_1^s and k_{-1}^s are the rate constants of the $R \rightarrow S$ and $S \rightarrow R$ interconversion in the stationary phase, respectively.

inert environment. Therefore, multidimensional techniques employing different columns in series in HPLC [101], CE [91,125], and GC [35,37,40] have been introduced. Stop-flow interconversion in a column series operated under multidimensional conditions, is typically performed in a series of three columns. The first and the third columns are chiral and the second column is achiral or an empty tube. After complete separation of the enantiomers in the first chiral column, at a temperature where enantiomerization is suppressed, one or both enantiomers are introduced to the second column using a heart-cut technique. Then the flow is stopped in this column and enantiomerization is performed at a chosen temperature and reaction time, *t*. Afterwards, the flow of the mobile phase introduces the enantiomers to the third column where they are separated [4]. The kinetic parameters and the enantiomerization barriers of both enantiomers are calculated as in the single-column method from the corresponding peak areas (A), the enantiomerization time (t), and the enantiomerization temperature (T).

3.3. Interconversion occurring during the separation process

If interconversion occurs at a suitable rate during the separation on the column, both the separation and the interconversion processes occur simultaneously. Interconversion of the pure enantiomer during the enantioselective separation process yields a peak cluster consisting of a peak of unconverted enantiomer and a hump formed by the interconverted species. Fig. 4 shows the peak clusters obtained by the on-column interconversion of thermally labile enantiomers *R* (Fig. 4A) and *S* (Fig. 4B).

The on-column interconversion of a racemic mixture during the separation process yields a peak cluster consisting of two peaks of nonconverted enantiomers and a plateau formed by the species that undergo at least one interconversion event (Fig. 4C).

The peak characteristics (retention times, areas, heights, widths and shapes) and the height of the plateau depend both on the analyte interconversion kinetics (determined by the prevailing temperature) as well as the separation system (type of chiral selector and the mobile phase flow-rate) [4,139].

Considering the equal mass or molar response factors for both enantiomers of conventional chromatographic detectors, the rate constants may be calculated directly from the peak areas of the *R* and *S* enantiomers prior to ($A_{R,0}$, $A_{S,0}$) and after the interconversion (A_R, A_S).

The following procedures have been used to calculate kinetic data and interconversion energy barriers from chromatograms obtained by the separation enantiomers that interconverted during the separation process: (i) methods based on a computer assisted simulation of chromatograms [4,21,131, 137,138], (ii) stochastic methods [139], (iii) methods based on approximation functions and (iv) deconvolution methods [8,42,43].

3.3.1. Computer assisted simulation of chromatograms

The determination of kinetic data from chromatograms obtained when separating enantiomers that interconverted during the separation process can be achieved by determining the best fit of computer simulated data and the real chromatogram. The simulation procedure that is most often used is based on the discontinuous theoretical plate model described by Schurig and co-workers. The first simulation program was introduced by Bürkle et al. [15], and later modified by Jung and Schurig [21,141] and Trapp and Schurig [138].

3.3.1.1. Theoretical plate model

TPM describes the chromatographic separation as a discontinuous process, assuming that all steps proceed repeatedly on each theoretical plate. Three steps are performed in every plate: (i) distribution of the *R* and *S* enantiomers between the two phases, (ii) the enantiomerization process in both phases, and finally (iii) shifting of the mobile phase to the next theoretical plate (cf. Fig. 3) [4,15].

Processes occurring in a theoretical plate during on-column interconversion are similar to those accomplished in the single-column stop-flow method and therefore Fig. 3 can be used to describe them.

The distribution of *R* and *S* enantiomers between the mobile phase (m) and the stationary phase (st) is determined according to Eq. (4) and Eq. (5):

$$m_{R,m} = \frac{1}{1 + k_R}(m_{R0,\mathrm{m}} + m_{R0,\mathrm{st}}) \tag{4a}$$

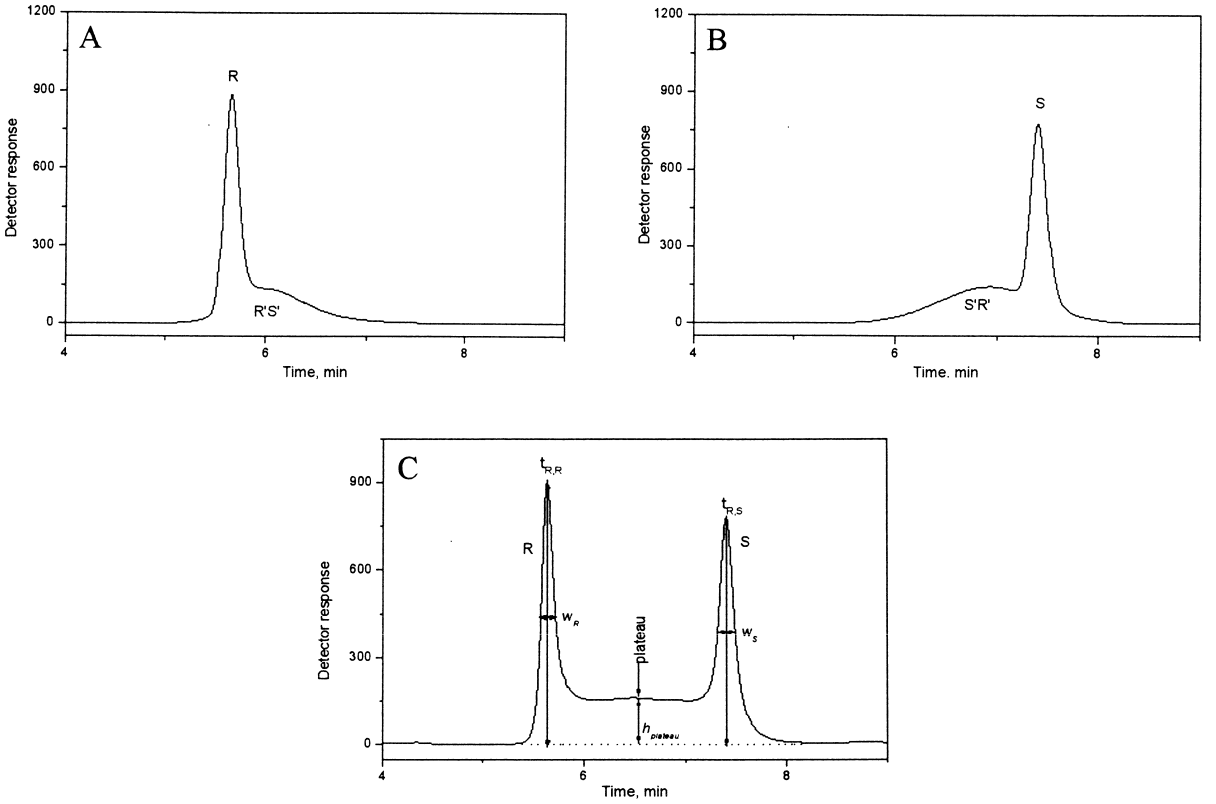

Fig. 4. Chromatogram obtained by the separation of racemic mixture of 1-chloro-2,2-dimethylaziridine enantiomers by two chiral columns coupled in series and working at different temperatures. $R'S'$ and $S'R'$ denotes interconverted species. Working conditions: 30 m × 0.25 mm FS capillary column coated with 0.125 μm film of heptakis(2,6-di-*O*-pentyl-3-trifluoroacetyl)-β-cyclodextrin was divided into two equal pieces (Chiral Dex B-TA ASTEC, Whippany, NJ, USA). The first half of the column was placed in the thermostat of HP 5890 II GC instrument (Hewlett-Packard, Avondale, USA). The second part was introduced via a heated tube into the Fractovap 4180 GC (Carlo Erba, Milan, Italy). Details on the working conditions shall be published separately [149].

$$m_{S,\mathrm{m}} = \frac{1}{1+k_S}(m_{S0,\mathrm{m}} + m_{S0,\mathrm{st}}) \tag{4b}$$

$$m_{R,\mathrm{st}} = \frac{k_R}{1+k_R}(m_{R0,\mathrm{m}} + m_{R0,\mathrm{st}}) \tag{5a}$$

$$m_{S,\mathrm{st}} = \frac{k_S}{1+k_S}(m_{S0,\mathrm{m}} + m_{S0,\mathrm{st}}) \tag{5b}$$

where $m_{R,\mathrm{m}}$, $m_{S,\mathrm{m}}$, $m_{R,\mathrm{st}}$ and $m_{S,\mathrm{st}}$ are the amounts of enantiomers R and S at equilibrium, $m_{R0,\mathrm{m}}$, $m_{S0,\mathrm{m}}$, $m_{R0,\mathrm{st}}$ and $m_{S0,\mathrm{st}}$ the amounts of R and S before equilibration, and k_R and k_S are the retention factors of the R and S enantiomers, calculated from the total retention time t_R and the mobile phase hold-up time t_M according to $k = (t_\mathrm{R}\text{-}t_\mathrm{M})/t_\mathrm{M}$, m denotes mobile and st stationary phases.

The interconversion process between the enantiomers during the residence time $\Delta t = t_\mathrm{M}/N$ in the chiral stationary phase and in the achiral mobile phase in a theoretical plate is determined by the respective rate constants. Since the forward and backward rate constants k^m in the mobile phase are equal, the equilibrium constant $K^\mathrm{m} = 1$, whereas the equilibrium constant in the chiral stationary phase depends on the two-phase partition coefficients $K_{\mathrm{D},R}$ and $K_{\mathrm{D},S}$

$$K^\mathrm{st} = \frac{k_1^\mathrm{st}}{k_{-1}^\mathrm{st}} = \frac{K_{\mathrm{D},S}}{K_{\mathrm{D},R}} = \frac{k_S}{k_R} \tag{6}$$

This equation implies that the backward rate constant k_{-1}^st is already determined for given values

of k_1^{st}, k_R and k_S and that k_1^{st} differs from k_{-1}^{st} when $k_S > k_R$, i.e. when the enantiomers are discriminated between, and hence separated in the presence of the chiral stationary phase $[-\Delta(\Delta G_{R\rightarrow S}) \neq 0]$.

The reversible first-order kinetics is described by:

$$\frac{dm_x}{dt} = k_1^{st}(m_{R,0} - m_x) - k_{-1}^{st}(m_{S,0} + m_x) \quad (7)$$

where the m are the masses of enantiomers (R, S) and interconverted species (x). The amount of m_x arises by interconversion of R and S.

Eq. (7) is solved by numerical integration, using the initial conditions:

$$m_R = \frac{k_{-1}^{st}}{k_1^{st} + k_{-1}^{st}} \cdot (m_{R,0} + m_{S,0}) + \frac{k_1^{st} m_{R,0} - k_{-1}^{st} m_{S,0}}{k_1^{st} + k_{-1}^{st}} \exp\left[-\left(k_1^{st} + k_{-1}^{st}\right)\right]\Delta t \quad (8)$$

The mass m_S is calculated from the mass balance $m_{R,0} + m_{S,0} = m_R + m_S$.

Assuming that the rate constants in the mobile and stationary phase are equal as a first approximation, the overall or apparent rate constants k_1^{app} and k_{-1}^{app} are calculated according to Eq. (9a) and (9b), respectively.

$$k_1^{app} = \frac{1}{1 + k_R} k^m + \frac{k_R}{1 + k_R} k_1^{st} \quad (9a)$$

$$k_{-1}^{app} = \frac{1}{1 + k_S} \cdot k^m + \frac{k_S}{1 + k_S} \cdot k_{-1}^{st} \quad (9b)$$

After these two steps, the content of the mobile phase is shifted to the subsequent theoretical plate, whereas the analytes in the stationary phase are retained. While a specific amount of the enantiomers is initially introduced in the first theoretical plate, the content of the mobile phase of the last theoretical plate is finally recorded as a chromatogram featuring an interconversion profile over time t. The rate constant and the kinetic activation parameters of enantiomerization are obtained by iterative comparison of experimental and simulated chromatograms. The best fit between simulated and experimental interconversion profiles provides the kinetic parameters and the energy barrier [4,15,21,138]. Fig. 5 shows experimental and simulated chromatograms of oxazepam separated by HPLC on a teicoplain column (Chirobiotic T, ASTEC) at different temperatures.

HRGC, HPLC and SFC chromatography as well as capillary electromigration methods (CEM) have been used to determine rate constants and energy barriers to interconversion using this method. The obtained results were in good agreement with those found by independent techniques [4].

3.3.2. Stochastic model

The stochastic model (SM), developed by Keller and Giddings [142], describes the chromatographic separation using time-dependent distribution functions Φ with the input parameters hold-up time t_M, retention times $t_{R,R}$ and $t_{R,S}$ and theoretical plate numbers N_R and N_S. The elution profile $P(t)$ calculated for an enantiomerization process during the separation is given by the sum of the distribution functions $\Phi_{R'}(t)$ and $\Phi_{S'}(t)$ of the noninterconverted enantiomers R' and S' and the probability density functions $\Psi_{R''}(t,t')$ and $\Psi_{S''}(t,t')$ of the interconverted enantiomers R'' and S'':

$$P(t) = \Phi_{R'}(t) + \Phi_{S'}(t) + \Psi_{R''}(t,t'') + \Psi_{S'''}(t,t'') \quad (10)$$

For the whole process, the mass balance $m_R + m_S = m_{R'} + m_{S'} + m_{R''} + m_{S''}$ must be fulfilled [139].

As in other methods, only apparent rate constants for the forward and backward reaction (k_1^{app} and k_{-1}^{app}) are obtained [139].

In the first step, the remaining concentrations of the noninterconverted enantiomers R' and S' are calculated according to an irreversible first-order reaction with the total retention times $t_{R,A}$ and $t_{R,B}$ as the reaction time:

$$c_R''(t_{R,R}) = c_{R,0} \exp\left(-k_1^{app} t_{R,R}\right) \quad (11a)$$

$$c_S''(t_{R,S}) = c_{S,0} \exp\left(-k_{-1}^{app} t_{R,S}\right) \quad (11b)$$

The concentration profiles of the antipode peaks approach a Gaussian distribution if the chromatographic conditions are linear. The standard deviation of the Gaussian distribution function is calculated from the plate number, N, or the peak width at half height, w_h:

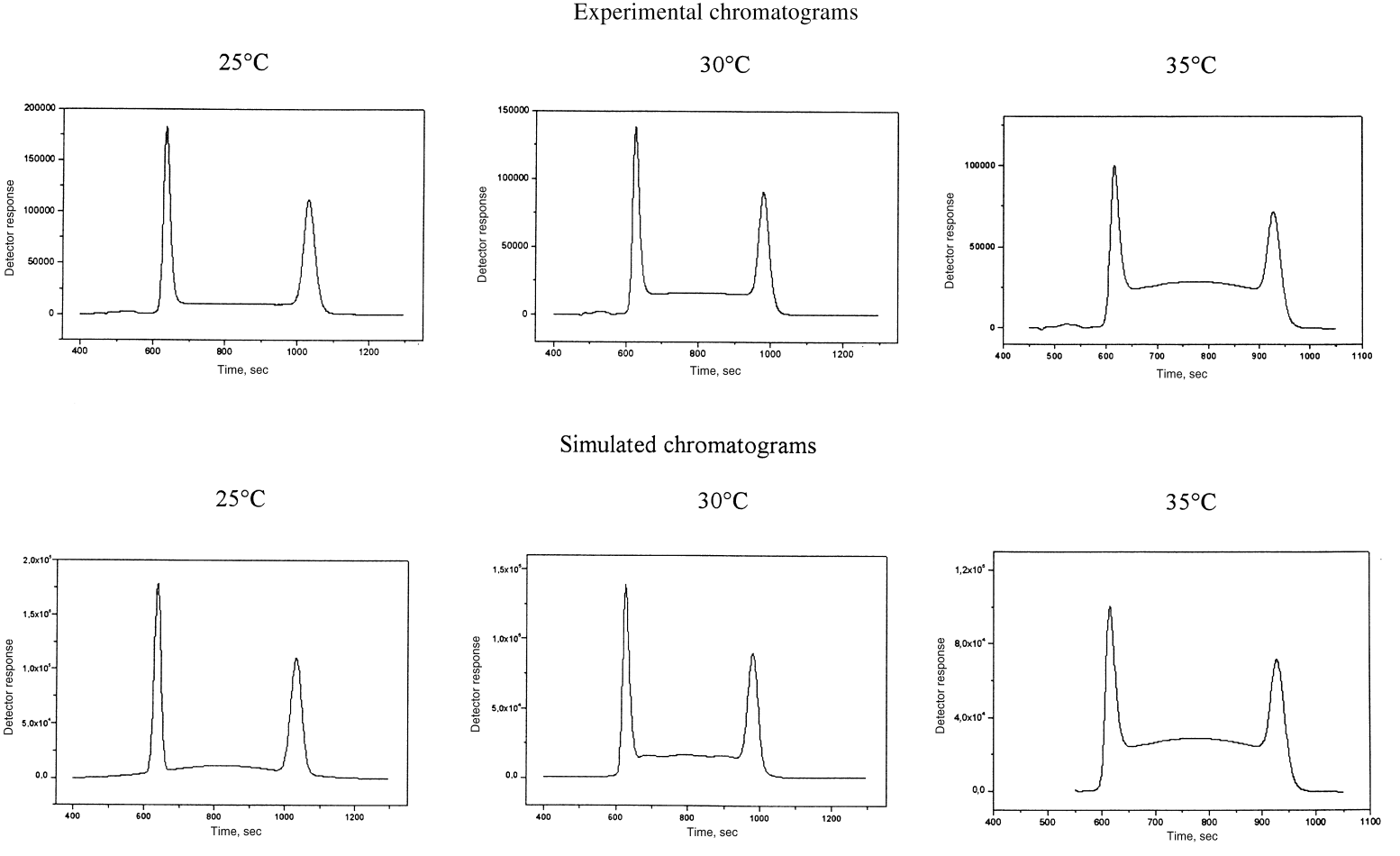

Fig. 5. Experimental and simulated chromatograms of oxazepam separated by HPLC on Chirobiotic T (CHT) column at different temperatures. CHT column (Chirobiotic T 250×4 mm I.D, ASTEC), mobile phase: methanol (with addition of 0.1% of acetic acid and 0.1% of TEA) and ethanol (with addition of 0.5% TFA and 0.5%TEA) (60:15, v/v), flow-rate 1.2 ml/min. UV detector at 254 nm.

$$\sigma^2 = \frac{t_R^2}{N} \tag{12a}$$

$$\sigma = \frac{w_h}{\sqrt{8 \ln 2}} \tag{13b}$$

It seems to be a contradiction to use plate numbers in a stochastic distribution model, but the plate number is employed here to characterize the sequence of partition steps during which the equilibrium, described by the partition coefficients K_D, is not reached completely because of the continuous mass transport by the mobile phase in a perpendicular direction [139]. To compute the profiles of the noninterconverted enantiomers R' and S',the time-dependent Gaussian distribution function $\Phi(t)$ is employed:

$$\Phi(t,t_{R,R}, \sigma_R, c'_R) = \sum \frac{c'_R}{\sigma_R \sqrt{2\pi}} \exp\left(-\frac{(t - t_{R,R})^2}{2\sigma_R^2} \right) \tag{14a}$$

$$\Phi(t,t_{R,S}, \sigma_S, c'_S) = \sum \frac{c'_S}{\sigma_S \sqrt{2\pi}} \exp\left(-\frac{(t - t_{R,S})^2}{2\sigma_S^2} \right) \tag{14b}$$

The concentration profile of the interconverted enantiomers R'' and S'' is calculated according to the derivations of Keller and Giddings [142], Kramer [143] and Cremer and Kramer [144]. The input parameters required for the calculation are the total retention times of the enantiomers $t_{R,R}$ and $t_{R,S}$, the apparent rate constants k_1^{app} and k_{-1}^{app}, and the initial concentration of the enantiomers. This procedure, however, describes only a concentration profile valid for ideal and linear chromatography. Hence, a distribution function, that fits theoretical plate theory and the solution of the mass balance equation of neat components, respectively, has to be used to consider phenomena like peak broadening and tailing. By integration over all distribution curves, a concentration profile $\Phi(t,t')$ was obtained which complies with the elution profile in nonideal linear chromatography [139].

3.3.3. Approximation function

Trapp and Schurig [139] derived an empirical approximation function that is based on the stochastic model. This allows the direct calculation of enantiomerization rate constants (k_1 and k_{-1}) and the Gibbs activation energies of enantiomerization, (ΔG^{app}) from chromatographic parameters, i.e. retention times of the enantiomers A and B (t_{RA} and t_{RB}), peak widths at half height (w_A and w_B) and the relative plateau height ($h_{plateau}$) [139]. The enantiomerization rate constants, obtained with this approximation function, have been validated by comparison with a simulated dataset of 15625 chromatograms. The mean, standard deviation and confidence interval showed a high correlation between the approximated and simulated rate constants. The average deviation from the Gibbs activation enthalpy of enantiomerization, ΔG^{app}, has been estimated to be as small as about ± 0.11 RT [139].

3.3.4. Deconvolution methods

From the previous sections, it is apparent that the chromatogram obtained by the dynamic separation of thermally labile enantiomers is very complex as there are peaks of the original *R*- and *S*-enantiomers highly overlapped with the interconverted species. For the direct calculation of kinetic data and interconversion energy barriers, however, peak characteristics (peak areas *A*, and retention times) of the original enantiomers are needed. Peak data from overlapped peaks can be obtained by:

(i) multidimensional systems combining two or more single separation systems [47]

(ii) the combination of two or more detectors [8–12,64,94]

(iii) computer assisted deconvolution methods [44,45,48,50,51].

3.3.4.1. Multidimensional systems

Marriott et al. [47] have studied the dynamic chromatographic interconversion of *E* and *Z* forms of oximes by using a novel cryogenic modulation method in a two-dimensional gas chromatographic separation system. The primary column was a conventional capillary GC column on which the molecular interconversion proceeds. In this case, the molecular dynamical process leads to a peak profile which contains information on the kinetics and thermodynamics of the interconverting molecules during chromatographic elution. There is an interconversion region between the peaks of the individual stereo-

isomers of the reaction. The infinitesimal profiles of interconversion along the entire column cannot be experimentally observed. Therefore, the total profile is subjected to mathematical modeling studies in order to match experiment with theory, and to gain the kinetic parameters of the process. An instantaneous ratio of the individual isomers was found during the chromatographic elution by direct measurement [47]. This was achieved by using a cryogenic zone focusing process, with rapid longitudinal modulation of a cold trap and continual pulsing of the collected zones into a fast-analysis high-resolution capillary column on which isomer interconversion was suppressed. The data were displayed as a two-dimensional contour plot to demonstrate the individual isomer profiles. The two-dimensional analysis also allows easy measurement of the peak ratios of the two isomers, which is an indicator of the extent of interconversion that has taken place. This also could be used to calculate the kinetic activation parameters and the enantiomerization energy barrier. Two model systems, acetaldoxime and butyraldoxime, were chosen to illustrate the use of the cryogenic modulation procedure. It has been anticipated that the procedure could be applied to other molecules, which undergo reversible reactions during the separation process [47].

3.3.4.2. Combination of two or more detectors

Combinations of spectral (UV spectrometry) and chirooptic detection (polarimetry and circular dichroism) have been used to study the dynamic chiral HPLC separation of enantiomers of thermally labile compounds [8–12,64,93,95]. The peak characteristics (peak areas and retention times) of noninterconverted enantiomers found by chirooptic detectors were, however, highly impacted with interconverted species. Thus the determination of kinetic activation parameters and interconversion energy barriers were found by a stochastic method evaluating chromatograms registered with a UV detector.

3.3.4.3. Computer-assisted deconvolution methods

The aim of any peak deconvolution procedure in chiral chromatography is to determine peak areas and peak retention times of enantiomers in a peak cluster on an experimental chromatogram. The use of this method in dynamic separation techniques, therefore, does not require any knowledge of separation mechanisms. For computer assisted peak deconvolution of complex chromatograms various software can be used. The number of peaks and design of peak shapes belong to basic input parameters in the peak deconvolution procedures. It is a problem to determine initial peak parameters for a deconvolution procedure for an overlapped peak cluster, particularly if the number of peaks present in the selected part of the chromatogram is not known.

3.3.4.3.1. *Estimation of the minimum peak number in the peak cluster* The number of apparent peaks is usually lower than the total number of peaks present in the recording obtained by the dynamic separation of thermally labile enantiomers. This is caused by extensive peak overlap, where the peaks differ only slightly in retention time. As a consequence no inflection points are observed for such peaks and the estimation of the total number of peaks in a chromatogram must be accomplished with another procedure. The number of peaks in a real chromatogram can be estimated from the dependence of the sum of squared errors between the experimental and deconvoluted chromatograms on the number of peaks considered [145]. A procedure for peak number estimation in a peak cluster obtained by dynamic SFC separation of oxazepam on a teicoplanin CSP at 35 °C using commercial peak-fitting program is illustrated below [146,147]. Peak type profiles (Gaussian, Lorenzian and exponentially modified Gaussian), estimated number of peaks, and the estimated peak centers and heights are the input parameters in the peak fitting program. The program is then optimized with other parameters to get the minimum of the function:

$$\mathrm{CHI}^2 = \sum_{i=1}^{N} \left[Y(x,t_i) + B(t_i) - Y_{\mathrm{exp}}(t_i) \right]^2 \qquad (15)$$

As the number of estimated peaks in the chromatogram increases, the resulting sum of the squared errors will decrease. The CHI^2 value is among the peak parameters accessible in the output of the peak fitting software. Fig. 6 shows original and deconvoluted peak clusters for two (A), three (B), four (C), five (D) six (E) and seven (F) estimated peaks in the considered peak cluster. The dependence CHI^2 on the number of fitted peaks is depicted in Fig. 7. This figure shows the break for three peaks. Any further

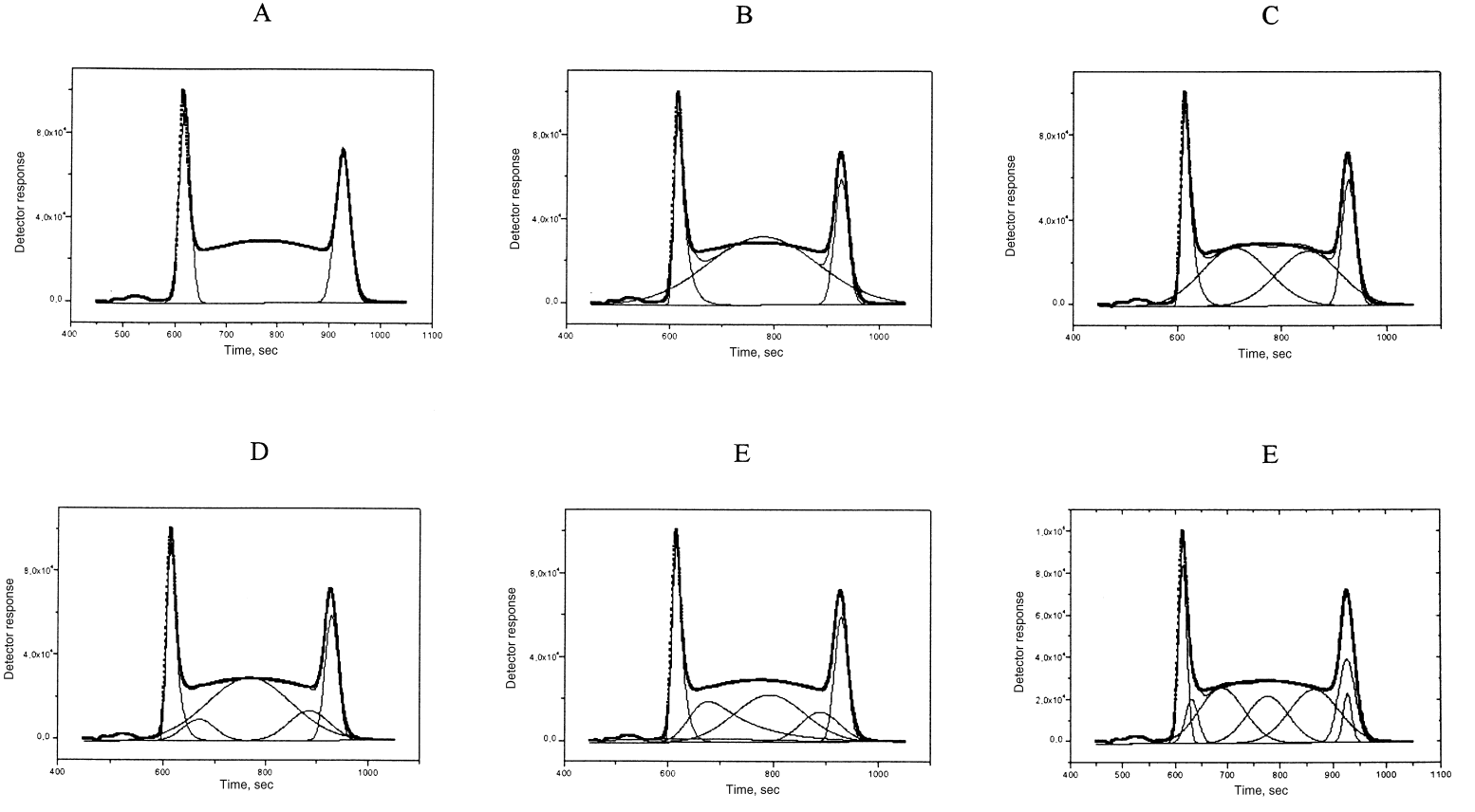

Fig. 6. Original and deconvoluted peak clusters for two (A), three (B), four (C), five (D) six (E) and seven (F) estimated peaks in the peak cluster obtained by the separation of lorazepam enatiomers on Chirobiotic T column at 35 °C. For others details see text below Fig. 5.

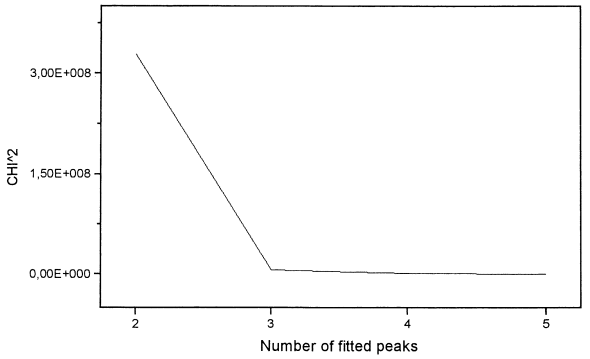

Fig. 7. Dependence of CHI^2 on the number of fitted peaks as found by computer assisted deconvolution of chromatogram obtained by separation of oxazepam enantiomers on Chirobiotic T column at 35 °C. For details see caption to Fig. 5.

increase in the number of peaks does not significantly decrease errors between the original and fitted peak cluster. That is why the use of three peaks is usually sufficient for the deconvolution of these peak clusters. For more precise peak fitting procedures we have used four peaks as this number is more realistic as follows from Fig. 4.

3.3.4.3.2. *Models used for peak fitting* Gaussian model: Various functions can be used for fitting. The Gaussian model describes a bell-shaped curve like the normal (Gaussian) probability distribution function, which can be expressed by the equation:

$$y = y_0 + \frac{A}{w\sqrt{\pi/2}} \cdot \exp\left(-\frac{2(t - t_R)^2}{w^2} \right) \quad (16)$$

where y_0 is the baseline offset, A is the peak area, $w = 2\sigma$, (approximately 0.849 of the peak width at half height) t is the time, t_R the retention time, σ half peak width at peak inflexion point (peak standard deviation) [146–148].

Exponentially modified Gaussian model (EMG): few chromatographic peaks are perfectly Gaussian, and this led to considerable effort, since 1959, to find a better peak model [148]. The exponentially modified Gaussian, or EMG function, gives good agreement between theory and experiment in many real cases. It is a Gaussian function convoluted (bent) onto an exponential axis of time constant, τ. The equation for the EMG function can be expressed in several ways. A typical example is the following equation:

$$y = y_0 + \frac{A}{\tau} \cdot \exp\left[\frac{1}{2}\left(\frac{\sigma}{\tau}\right)^2 - \left(\frac{t - t_R}{\tau}\right) \right] \cdot \int_{-\infty}^{z/\sqrt{2}} \exp(-t^2)\mathrm{d}t \quad (17)$$

where A is the peak area, $z = \{(t - t_R)/\sigma - \sigma/\tau\}$, t is the time, t_R the retention time, σ the standard deviation and τ the time constant of the peak asymmetry. Both Gaussian and EMG functions are accessible in many softwares used for deconvolution of overlapped peaks [146–148].

3.4. Determination of the interconversion energy barrier

The energy barriers to $R \rightarrow S$ and $S \rightarrow R$ interconversion can be found from the apparent rate constants for the $R \rightarrow S$ (k_1^{app}) and $S \rightarrow R$ (k_{-1}^{app}) enantiomerization using the Eyring equation [140]:

$$-\Delta G_{R\rightarrow S}^{app} = RT \ln\left(\frac{hk_1^{app}}{\kappa k_b T}\right) \quad (18a)$$

or

$$-\Delta G_{S\rightarrow R}^{app} = RT \ln\left(\frac{hk_{-1}^{app}}{\kappa k_b T}\right) \quad (18b)$$

where R is the universal gas constant, T is the temperature in K, κ is transmission coefficient, k_b is the Boltzmann constant and h is Planck's constant.

Tables 1–4 show the rate constants and energy barriers determined for some 3-hydroxy-1,4-benzodiazepine drugs by DHPLC, DSFC and DMEKC.

Table 1
Apparent rate constants (k_1^{app},k_{-1}^{app}) and energy barrier to enantiomerization ($\Delta G_{A\rightarrow B}^{app}$and $\Delta G_{B\rightarrow A}^{app}$) determined for lorazepam by DSFC and HPLC on studied columns at 45°C

Column	Rate constant (s^{-1})		Energy barrier (kJ mol^{-1})	
	k_1^{app}	k_{-1}^{app}	$\Delta G_{A\rightarrow B}^{app}$	$\Delta G_{B\rightarrow A}^{app}$
CHR SFC	$4.32\cdot10^{-3}$	$4.29\cdot10^{-3}$	−87.6	−87.7
CHT1 HPLC	$4.03\cdot10^{-3}$	$3.10\cdot10^{-3}$	−87.9	−88.6
CHT2 HPLC	$3.97\cdot10^{-3}$	$3.20\cdot10^{-3}$	−87.9	−88.5
CHT SFC	$4.28\cdot10^{-3}$	$2.18\cdot10^{-3}$	−87.8	−89.5
CHV SFC	$2.55\cdot10^{-3}$	$2.60\cdot10^{-3}$	−89.1	−89.0
WH HPLC	$6.31\cdot10^{-4}$	$6.83\cdot10^{-4}$	−92.7	−92.45

Table 2
Apparent rate constants (k_1^{app},k_{-1}^{app}) and energy barrier to enantiomerization ($\Delta G_{A\to B}^{app}$and $\Delta G_{B\to A}^{app}$) determined for lormetazepam by DSFC and HPLC on studied columns at 45 °C

Column	Rate constant (s^{-1})		Energy barrier (kJ mol^{-1})	
	k_1^{app}	k_{-1}^{app}	$\Delta G_{A\to B}^{app}$	$\Delta G_{B\to A}^{app}$
CHR SFC	$7.30\cdot10^{-4}$	$9.58\cdot10^{-4}$	−92.3	−91.6
CHT HPLC	$9.44\cdot10^{-4}$	$8.54\cdot10^{-4}$	−91.6	−91.9
CHT SFC	$1.02\cdot10^{-3}$	$1.04\cdot10^{-3}$	−91.4	−91.4
CHV SFC	$1.32\cdot10^{-3}$	$1.22\cdot10^{-3}$	−90.8	−91.0
WH SFC	$2.12\cdot10^{-3}$	$1.97\cdot10^{-3}$	−89.4	−90.0
WH HPLC	$2.90\cdot10^{-4}$	$2.81\cdot10^{-4}$	−93.3	−93.4

Table 3
Apparent rate constants (k_1^{app},k_{-1}^{app}) and energy barrier to enantiomerization ($\Delta G_{A\to B}^{app}$and $\Delta G_{B\to A}^{app}$) determined for oxazepam by DSFC and HPLC on studied columns at 45 °C

Column	Rate constant (s^{-1})		Energy barrier (kJ mol^{-1})	
	k_1^{app}	k_{-1}^{app}	$\Delta G_{A\to B}^{app}$	$\Delta G_{B\to A}^{app}$
CHR SFC	$7.08\cdot10^{-4}$	$1.02\cdot10^{-3}$	−92.4	−91.4
CHT1 HPLC	$3.57\cdot10^{-3}$	$3.20\cdot10^{-3}$	−88.2	−88.5
CHT2 HPLC	$5.38\cdot10^{-4}$	$4.05\cdot10^{-3}$	−87.2	−87.9
CHT SFC	$6.72\cdot10^{-3}$	$2.95\cdot10^{-3}$	−86.6	−88.7
CHV SFC	$4.75\cdot10^{-3}$	$4.92\cdot10^{-3}$	−87.5	−87.4
WH HPLC	$7.01\cdot10^{-4}$	$6.51\cdot10^{-4}$	−92.4	−92.6

The peak characteristics (retention times and peak areas) needed for the calculation of data listed in Tables 1–4 were found by computer assisted deconvolution of the peak clusters depicted in Figs. 8 and 9 using both three and four peak concepts. Gaussian and/or EMG models were used in the fitting procedure.

Calculations of the energy barriers to enantiomerization were accomplished by using Eqs. (18a) and (18b). As the configurations of peaks on the chromatograms were not known, instead of configurations *R* and *S*, the letters A and B were used in Tables 1–4. An arbitrarily refers to the first eluted, and B to the second eluted enantiomer. Transmission coefficient $\kappa = 0.5$ was substituted in Eq. (18) in correspondence with a value used in literature [130,131]. However, transmission coefficient can be determined by the slope of the linear dependence:

$$\ln\left(\frac{k_1^{app}}{T}\right) = \ln\left(\kappa\frac{k_B}{h}\right) - \frac{\Delta G_{A\to B}^{app}}{RT} \quad (19)$$

which is obtained by the rearrangement of Eq. (18a) for enantiomers where the configuration is not known.

Table 4
Apparent rate constants (k_1^{app},k_{-1}^{app}) and energy barrier to enantiomerization ($\Delta G_{A\to B}^{app}$ and $\Delta G_{B\to A}^{app}$) determined for lorazepam, temazepam and oxazepam by CE at 25 °C [149]

Column	Rate constant (s^{-1})		Energy barrier (kJ mol^{-1})	
	k_1^{app}	k_{-1}^{app}	$\Delta G_{A\to B}^{app}$	$\Delta G_{B\to A}^{app}$
Lorazepam	$4.14\cdot10^{-4}$	$3.96\cdot10^{-4}$	−93.7	−93.8
Temazepam	$6.21\cdot10^{-4}$	$6.18\cdot10^{-4}$	−92.7	−92.7
Oxazepam	$1.32\cdot10^{-3}$	$1.32\cdot10^{-3}$	−90.8	−90.8

Fig. 10 shows the dependence of $\ln(k/T)$ on $1/T$ obtained for the first eluted enantiomer of lorazepam separated on a (R,R)-Whelk O1 column by SFC at temperature intervals between 35 and 60 °C. Evaluation of the dependence shown in Fig. 10 gives the value $\kappa = 0.27$. This number indicates that the interconversion of configurational enantiomers is more complex than conformational ones.

Eqs. (18a) and (18b) are used to calculate energy barriers to enantiomerization from the chromatographic data. If enantiomers are separated and interconverted on a chiral column simultaneously, interconversion times of both enantiomers are different. This is supposed to be the reason for different apparent kinetic activation parameters and interconversion energy barriers for enantiomers.

The dependence of the apparent enantiomerization barrier ($\Delta G_{A\to B}^{app}$, $\Delta G_{B\to A}^{app}$) on temperature can be used for the calculation of the apparent activation enthalpy ($\Delta H_{A\to B}^{app}$, $\Delta H_{B\to A}^{app}$) and entropy ($\Delta S_{A\to B}^{app}$, $\Delta S_{B\to A}^{app}$) using the Gibbs–Helmholz equation:

$$\Delta G_{A\to B}^{app} = \Delta H_{A\to B}^{app} - T\Delta S_{A\to B}^{app} \quad (20a)$$

or

$$\Delta G_{B\to A}^{app} = \Delta H_{B\to A}^{app} - T\Delta S_{B\to A}^{app} \quad (20b)$$

From the above equations, it follows that the enantioselectivity of a chiral selector is responsible for differences in the thermodynamic parameters for both enantiomers. Difference in the activation energy is proportional to the enantioselectivity (α) as per the following equation:

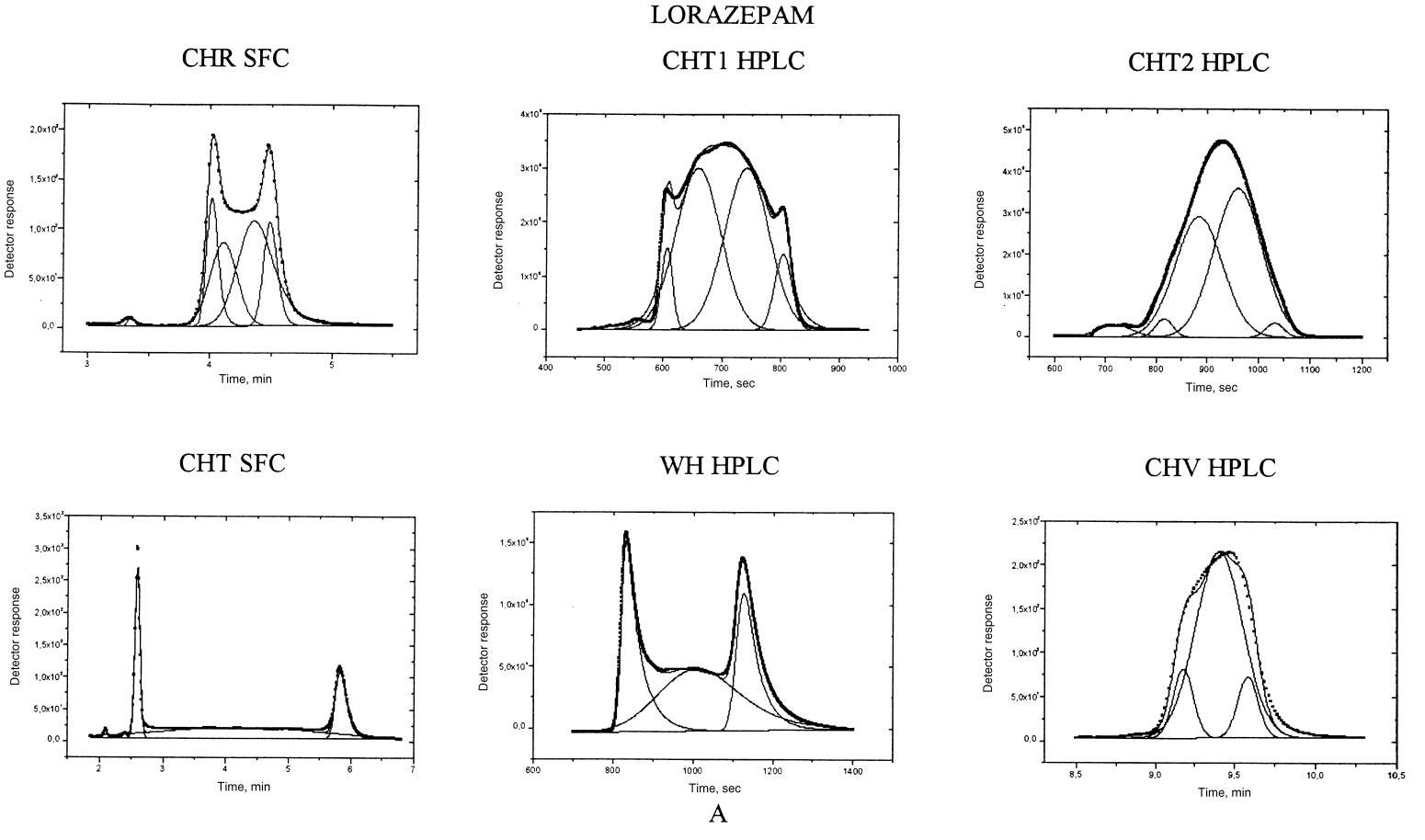

Fig. 8. Original peak clusters and peaks found by a computer assisted deconvolution of peak clusters for lorazepam (A), lormetazepam (B) oxazepam (C) separated by HPLC and SFC at 45 °C. CHR–Chirobiotic R (Ristocetin), CHT–Chirobiotic T (Teicoplanin), CHV–Chirobiotic V (Vancomycin). Columns CHR, CHT and CHV (250×4 mm I.D) were purchased from ASTEC). WH–(R,R)-Whelk-O1 column (25 cm×0.46 cm I.D., 5 μm, Regis, Morton Grove, IL, USA). Details on all working conditions shall be published separately [149].

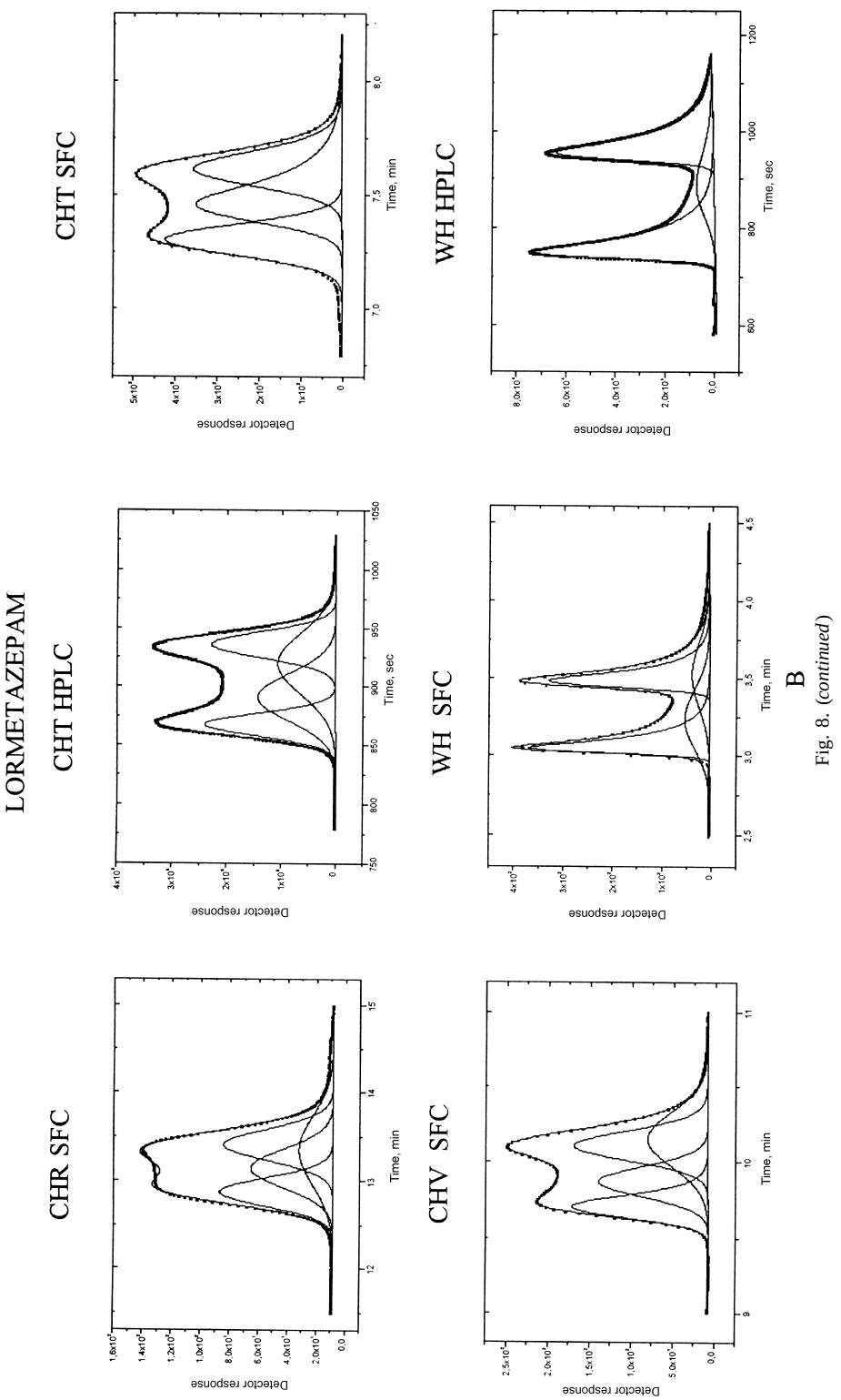

Fig. 8. (*continued*)

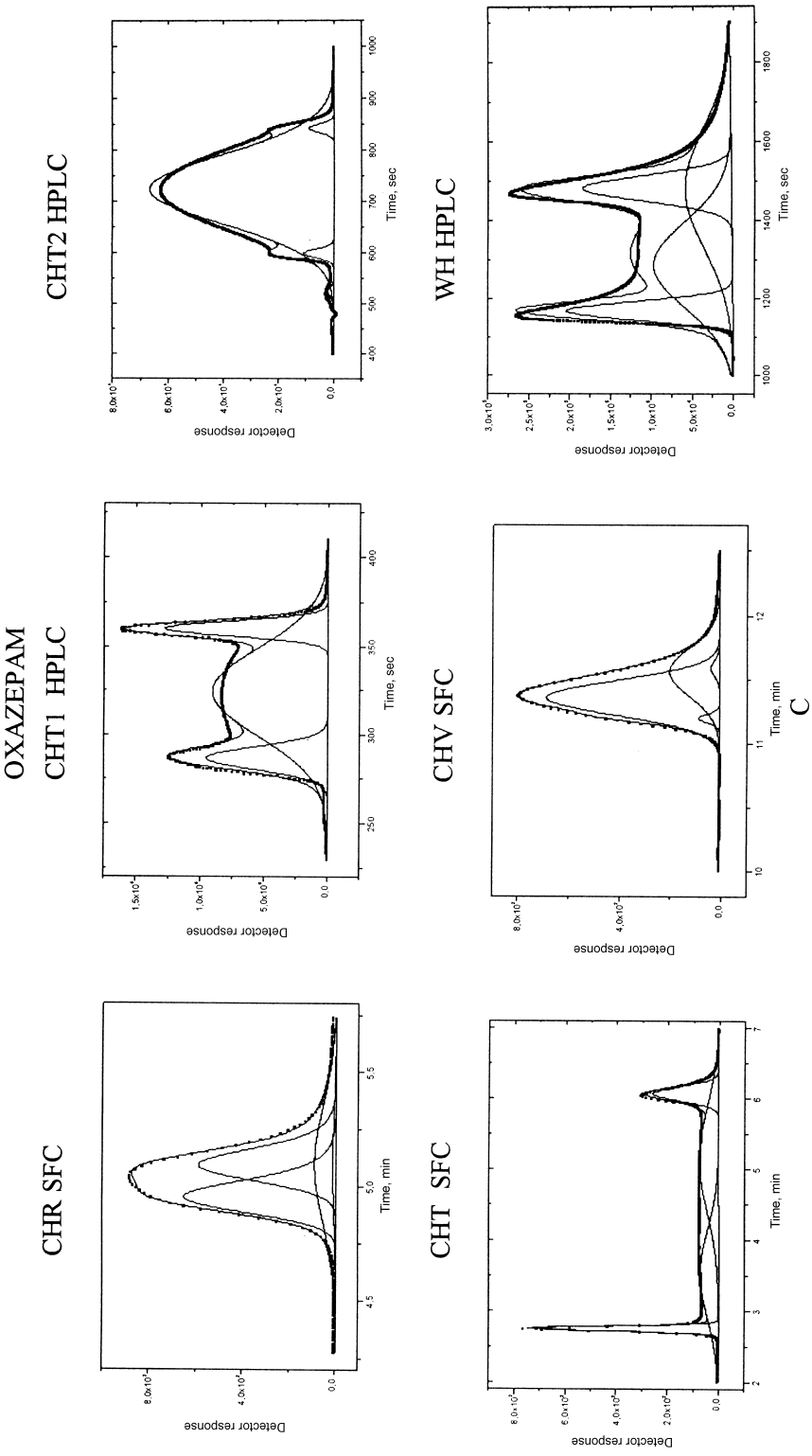

Fig. 8. (*continued*)

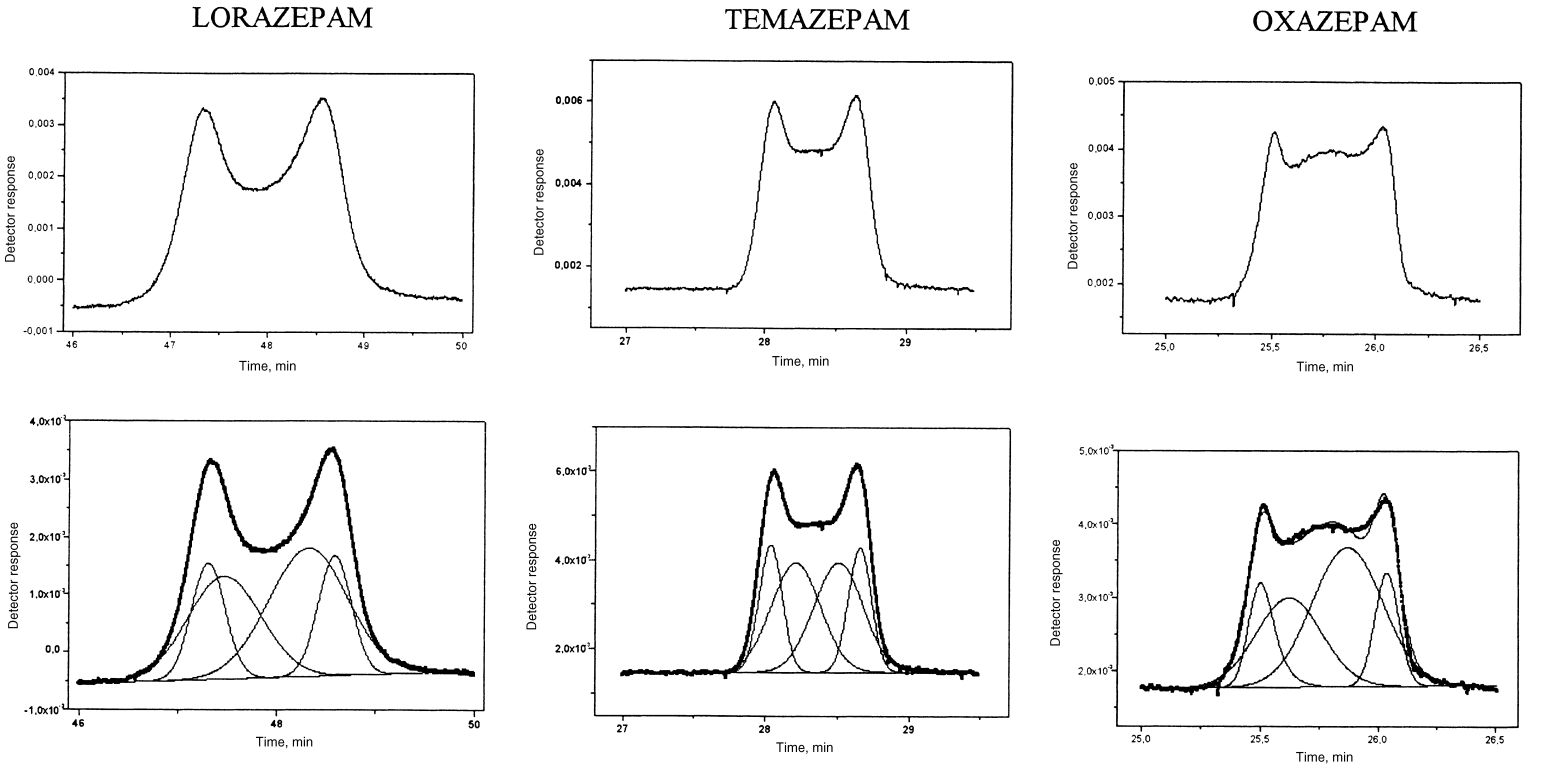

Fig. 9. Original peak clusters (upper records) and peaks found by a computer assisted deconvolution (bottom records) for lorazepam (A), temazepam (B) oxazepam (C) separated by CE at 25 °C. Details on all working conditions shall be published separately [149].

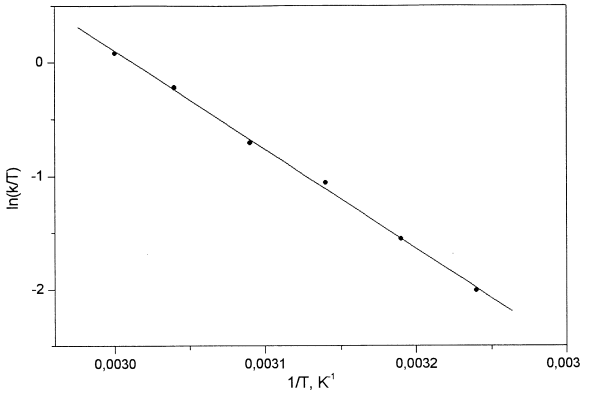

Fig. 10. Dependence of ln (k/T) on $1/T$ obtained for the first eluted enantiomer of lorazepam on (R,R)-Whelk O1 column by SFC at temperature interval 35–60 °C. Column WH–(R,R)-Whelk-O1 column (25 cm×0.46 cm I.D., 5 μm, Regis, Morton Grove, IL, USA). $F_m = 2$ ml min^{-1} of supercritical CO_2 with 12.5% methanol and 0,5% diethylamine as modifier. Details on all working conditions shall be published separately [149].

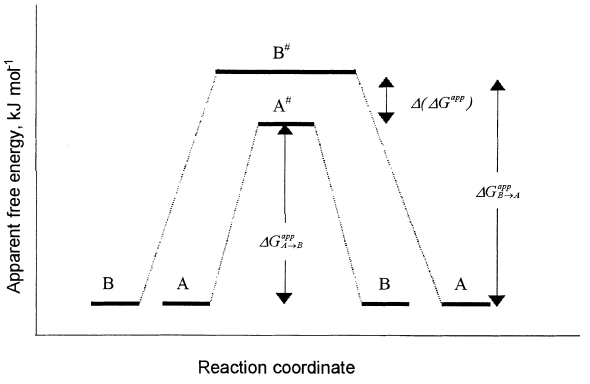

Fig. 11. Free energy interconversion coordinate diagram for the conversion of enantiomer $R \rightarrow S$ and $S \rightarrow R$.

$$\Delta(\Delta G^{\text{app}}) = \Delta G^{\text{app}}_{\text{B}\rightarrow\text{A}} - \Delta G^{\text{app}}_{\text{A}\rightarrow\text{B}} = -RT \ln \frac{k_{\text{B}}}{k_{\text{A}}} = RT \ln \alpha \quad (21)$$

Fig. 11 shows a free energy interconversion coordinate diagram for the enantioselective interconversion of enantiomer A→B and B→A. From Eq. (21) and Fig. 11 it follows that the more enantioselective a separation system, the higher the apparent enantiomerization barrier for the compound represented by the second eluted peak. This is why the apparent data calculated for the first eluted peak are less affected by the experimental conditions and to a first approximation they can be tabulated and compared with those data found by classical methods.

Data listed in Table 5 for 3-hydroxy-1,4-benzodiazepines shows very good consistency of enantiomerization energy barrier for lorazepam and temazepam (absolute difference of less than 1%) and acceptable consistency for temazepam (difference around 2.6% rel.) determined by DSFC [51] and DMEKC [130]. The different separation techniques and temperatures at which the data are compared in Table 5 can explain differences in enthalpic and entropic data [51].

4. Conclusion

Most known enantioselective separation methods can be utilized to determine the interconversion energy barriers of enantiomers. These include LC,GC, SFC, pseudophase CE, and CEC. The

Table 5
Kinetic activation parameters and interconversion energy barriers determined for lorazepam temazepam and oxazepam by DSFC* at 313 K [51] and DMEKC** at 293 K [130]

Compound	k_1^{app} (s^{-1})	$\Delta G^{\text{app}}_{\text{A}\rightarrow\text{B}}$ (kJ mol^{-1})	$\Delta H^{\text{app}}_{\text{A}\rightarrow\text{B}}$ (kJ mol^{-1})	$\Delta S^{\text{app}}_{\text{A}\rightarrow\text{B}}$ [J (K mol)$^{-1}$]
Lorazepam	$1.83\cdot10^{-3}$*	91.4*	68.2*	−40.6*
	$3.1\cdot10^{-4}$**	91.4**	76.5**	−50.9**
Temazepam	$6.73\cdot10^{-4}$*	94.0*	66.8*	−86.9*
	$2.9\cdot10^{-4}$**	91.6**	90.5**	−3.9**
Oxazepam	$2.15\cdot10^{-3}$*	91.0 *	59.9*	−100*
	$3.3\cdot10^{-4}$**	91.4**	72.0**	−65.8**

optional instrumental approach for a specific measurement is usually determined by the physicochemical properties of the analyte (e.g. vapor pressure, solubility, stability, detectability, etc.) as well as quality of the enantiomeric separation that can be achieved using a particular method. Sometimes more than one instrumental method can be used. Once the instrumental technique is selected, one or more of the seven possible operational approaches outlined in this overview must be chosen and used. Each of these approaches has certain advantages and disadvantages in terms of time of analysis, types of equipment and software required, accuracy and precision of data produced, and so forth. Given the number of separations-based instrumental and operational approaches, it is likely that one or more combinations can be found to effectively evaluate the interconversion of most enantiomers of interest to the scientific community.

Acknowledgements

I.K., P.O. and P.M. acknowledge the support of the Grant Agency of Slovak Republic (VEGA 1/9127/02)) and the Agency for International Science and Technology Cooperation in Slovakia (Grant No. 035/2001). D.W.A. gratefully acknowledges partial support of this work by the National Institutes of Health, NIH RO1 GM53825-07.

References

[1] FDA's policy statement for the development of new stereoisomeric drugs. Chirality 4 (1992) 338.
[2] V.Schurig, Buerkle, Zlatkis, Poole, Natturwischenschaften 66 (1979) 423.
[3] V. Schurig, W. Buerkle, J. Am. Chem. Soc. 47 (1982) 3850.
[4] O. Trapp, G. Schoetz, V. Schurig, Chirality 13 (2001) 403.
[5] V. Schurig, F. Keller, S. Reich, M. Fluck, Tetrahed. Asym. 8 (1997) 3475.
[6] R. Kiesswetter, T. Burgemeister, A. Mannschreck, Enantiomer 4 (1999) 289.
[7] G. Bringmann, M. Heubes, M. Breuning, L. Gobel, M. Ochse, B. Schoner, O. Schupp, J. Org. Chem. 65 (2000) 722.
[8] A. Mannschreck, D. Andert, E. Eiglsperger, E. Gmahl, H. Buchner, 25 (1988) 182.
[9] A. Mannschreck, L. Kiessel, Chromatographia 28 (1989) 263.
[10] C. Wolf, W.A. Koenig, C. Roussel, Liebigs Ann. (1995) 781.
[11] S. Allenmark, J. Oxelbark, Chirality 9 (1997) 638.
[12] T. Kusano, M. Tabatabai, Y. Okamoto, V. Boehmer, J. Am. Chem. Soc. 121 (1999) 3789.
[13] J. Oxelbark, S. Allenmark, J. Chem. Soc. Perkin Trans. 2 (1999) 1587.
[14] J. Kallen, E. Heilbronner, Helv. Chim. Acta 43 (1960) 489.
[15] W. Buerkle, H. Karfunkel, V. Schurig, J. Chromatogr. 288 (1984) 1.
[16] Y.-H. Lai, P.J. Marriott, B.-C. Tan, Aust. J. Chem. 38 (1985) 307.
[17] P.J. Marriott, Y.-H. Lai, Inorg. Chem. 25 (1986) 3680.
[18] P.J. Marriott, Y.-H. Lai, J. Chromatogr. 447 (1988) 29.
[19] V. Schurig, U. Leyer, Tetrahed. Asym. 1 (1990) 1.
[20] V. Schurig, D. Schmalzing, M. Schleimer, Angew Chem. Int. Ed. 30 (1991) 987.
[21] M. Jung, M. Schurig, J. Am. Chem. Soc. 114 (1992) 529.
[22] V. Schurig, M. Jung, M. Schleimer, F.-G. Klaerner, Chem. Ber. 125 (1992) 1301.
[23] M. Jung, M. Fluck, V. Schurig, Chirality 6 (1994) 510.
[24] P.J. Marriott, Y-H. Lai, Chem. Aust. (1994) 386.
[25] V. Schurig, A. Glausch, M. Fluck, Tetrahed. Asym. 6 (1995) 2161.
[26] C.H. Wolf, W.A. Koenig, C.H. Roussel, Liebigs Annalen 5 (1995) 781.
[27] D.H. Hochmuth, W.A. Koenig, Liebigs Ann. 33 (1996) 947.
[28] C. Wolf, D.H. Hochmuth, W.A. Koenig, C. Roussel, Liebigs Ann. 33 (1996) 357.
[29] C. Wolf, D.H. Hochmuth, W.A. Koenig, C. Roussel, Liebigs Ann. 33 (1996) 357.
[30] D.H. Hochmuth, W.A. Koenig, Liebigs Ann. 33 (1996) 947.
[31] P.U. Biedermann, V. Schurig, I. Agranat, Chirality 9 (1997) 350.
[32] V. Schurig, F. Keller, S. Reich, M. Fluck, Tetrahed. Asymmetry 8 (1997) 3475.
[33] P. Haglund, M. Harju, Organohalogen Comp. 31 (1997) 244.
[34] V. Schurig, S. Reich, Chirality 10 (1998) 425.
[35] V. Schurig, S. Reich, Chirality 10 (1998) 316.
[36] N.A. Katsanos, R. Thede, F. Roubani-Kalantzopoulou, J. Chromatogr. A 795 (1998) 133.
[37] S. Reich, V. Schurig, J. Microcol. Sep. 11 (1999) 475.
[38] S. Reich, V. Schurig, GIT Lab. J. 3 (1999) 39.
[39] M.T. Harju, P. Haglund, J. Anal. Chem. 364 (1999) 219.
[40] S. Reich, O. Trapp, V. Schurig, J. Chromatogr. A 892 (2000) 487.
[41] S. Reich, V. Schurig, in: P. Sandra, A.J. Rackstraw (Eds.), Proceedings of the 20th International Symposium on Capillary Chromatography, I.O.P.M.S. vzw., Kortrijk, Belgium, J.13, 1998.
[42] P. Trapp, V. Schurig, J. Am. Chem. Soc. 122 (2000) 1424.
[43] R.G. Kostyanovsky, G.K. Kadorkina, V.R. Kostyanovsky, V. Schurig, O. Trapp, Angew Chem. Int. Ed. 39 (2000) 2938.
[44] J. Krupcik, P. Oswald, I. Spanik, P. Majek, M. Bajdichova, P. Sandra, D.W. Armstrong, Analusis 28 (2000) 859.
[45] J. Krupcik, P. Oswald, I. Spanik, P. Majek, M. Bajdichova, P. Sandra, D.W. Armstrong, J. Microcol. Sep. 12 (2000) 630.

[46] O. Trapp, V. Schurig, Chem. Eur. J. 7 (2001) 1495.
[47] P. Marriott, O. Trapp, R. Shellie, V. Schurig, J. Chromatogr. A 919 (2001) 115.
[48] J. Krupčík, P. Oswald, K. Desmet, P. Sandra, D.W. Armstrong, in: Proceedings from the Symposium ACES II, University of Bayreuth October 8–10, 2001, p. 34.
[49] C. Wolf, W.H. Pirkle, C.J. Wetchm, D.H. Hochmuth, W.A. Koenig, G.-L. Chee, J.L. Charlton, J. Org. Chem. 62 (1997) 5208.
[50] P. Oswald, K. Desmet, P. Sandra, J. Krupcik, D.W. Armstrong, Chirality 14 (2002) 334.
[51] P. Oswald, K. Desmet, P. Sandra, J. Krupcik, D.W. Armstrong, J. Chromatogr. B 779 (2002) 283.
[52] I. Itusconi, G. Perseo, L. Franzoni, I.P.C. Montecucchhi, Naturwissenschaften 66 (1979) 423.
[53] M. Lebl, V. Gut, J. Chromatogr. 260 (1983) 478.
[54] M. Moriyasu, Y. Hashimoto, M. Endo, Bull. Chem. Soc. Jpn. 56 (1983) 1972.
[55] W.R. Melander, H.J. Lin, J. Jacobson, C. Horvath, J. Phys. Chem. 88 (1984) 4527.
[56] J. Jacobson, W. Melander, G. Vaisnys, C. Horvath, J. Phys. Chem. 88 (1984) 4536.
[57] H. Scheruebl, U. Fritzsche, A. Mannschreck, Chem. Ber. 117 (1984) 336.
[58] A. Eiglsperger, F. Kastner, A. Mannschreck, J. Mol. Struct. 126 (1985) 421.
[59] M. Moriyasu, K. Kawanishi, A. Kato, Y. Hashimoto, M. Sugiura, T. Sai, Bull. Chem. Soc. Jpn. 58 (1985) 3351.
[60] M. Mintas, Z. Orhanovic, K. Jakopcic, H. Koller, G. Stuehler, A. Mannschreck, Tetrahed. Assym. 41 (1985) 229.
[61] M.A. Cuyegkeng, A. Mannschreck, Chem. Ber. 120 (1987) 803.
[62] S.E. Biali, Z. Rappoport, A. Mannschreck, N. Pustet, Angew. Chem. 101 (1989) 202.
[63] J.C. Gesquiere, E. Diesis, M.T. Cung, A. Tartar, J. Chromatogr. 478 (1989) 121.
[64] A. Mannschreck, L. Kiessl, Chromatographia 28 (1989) 263.
[65] A. Mannschreck, H. Zinner, N. Pustet, Chimia 43 (1989) 165.
[66] B. Stephan, H. Zinner, F. Kastner, A. Mannschreck, Chimia 10 (1990) 336.
[67] J. Veciana, M.I. Crespo, Angew Chem. Int. Ed. 30 (1991) 74.
[68] J. Veciana, M.I. Crespo, Angew. Chem. 103 (1991) 85.
[69] J. Veciana, M.I. Crespo, Angew.Chem. Int. Ed. Engl. 30 (1991) 74.
[70] S. Friebe, G.J. Kraus, J. Chromatogr. 598 (1992) 139.
[71] W.H. Pirkle, C.I. Welch, B.O. Lamm, J. Org. Chem. 57 (1992) 3854.
[72] J. Vorkapic-Furac, M. Mintas, F. Kastner, A. Mannschreck, J. Heterocycl. Chem. 29 (1992) 327.
[73] E. Gur, Y. Kaida, Y. Okamoto, S.E. Biali, Z. Rappoport, J. Org. Chem. 57 (1992) 3689.
[74] L. Loncar, K. Otocan, M. Mintas, T. Troetsch, A. Mannschreck, Croat. Chem. Acta 66 (1993) 209.
[75] W.H. Pirkle, C.J. Welch, A.J. Zych, J. Chromatogr. 648 (1993) 101.
[76] W.H. Pirkle, C.J. Welch, Asymmetry 5 (1994) 777.
[77] A.Z.-Q. Khan, J. Sandstroem, J. Chem. Soc. Perkin Trans. 2 (1994) 1575.
[78] K. Cabera, D. Lubda, J. Chromatogr. A 666 (1994) 433.
[79] A. Wutte, G. Gibitz, S. Friebe, G.J. Krauss, J. Chromatogr. A 677 (1994) 186.
[80] S. Friebe, B. Hartrodt, K.-J. Neubert, G. Kraus, J. Chromatogr. A 661 (1994) 7.
[81] C. Villani, W.H. Pirkle, J. Chromatogr. A 693 (1995) 63.
[82] C. Villani, W.H. Pirkle, Tetrahed. Asym. 6 (1995) 27.
[83] C. Wolf, W.A. Koenig, C. Roussel, Chirality 7 (1995) 610.
[84] F. Gasparrini, L. Lunazzi, J. Org. Chem. 60 (1995) 5515.
[85] D. Casarini, L. Lunazzi, S. Alcaro, F. Gasrini, C. Villani, J. Org. Chem. 60 (1995) 5515.
[86] G.J. Terfloth, W.H. Pirkle, K.G. Lynam, E.C. Nicolas, J. Chromatogr. A 705 (1995) 185.
[87] R.J. Friary, M. Spangler, R. Ostermann, L. Schulman, J.H. Schwerdt, Chirality 8 (1996) 364.
[88] K. Cabrera, M. Jung, M. Fluck, V. Schurig, J. Chromatogr. A 731 (1996) 315.
[89] W.H. Pirkle, P.G. Murray, J. Chromatogr. A 719 (1996) 299.
[90] W.H. Pirkle, J.L. Brice, G.J. Terfloth, J. Chromatogr. A 753 (1996) 109.
[91] A. Bunke, T. Jira, T. Beyrich, J. Chromatogr. A 728 (1996) 441.
[92] R. Thede, D. Haberland, E. Below, J. Chromatogr. A 728 (1996) 401.
[93] L. Loncar-Tomaskovic, M. Mintas, T. Trotsch, A. Mannschreck, Enantiomer 2 (1997) 459.
[94] T. Nishikawa, Y. Hayashi, S. Suzuki, H. Kubo, H. Ohtani, J. Chromatogr. A 767 (1997) 93.
[95] S. Allenmark, J. Oxelbark, Chirality 9 (1997) 638.
[96] P. Haglund, M. Harju, Organohalogen Comp. 31 (1997) 244.
[97] R. Thede, E. Below, D. Haberland, S.H. Langer, Chromatographia 45 (1997) 149.
[98] C. Wolf, W.H. Pirkle, C.J. Welch, D.H. Hochmuth, W.A. Koenig, G.-L. Chee, J.L. Charlton, J. Org. Chem. 62 (1997) 5208.
[99] F. Gasparrini, D. Misiti, M. Pierini, C.C. Villani, Tetrahed. Asym. 8 (1997) 2069.
[100] R. Thede, D. Haberland, C. Fischer, J. Liq. Chromatogr. Rel. Technol. 21 (1998) 2089.
[101] K. Lorenz, E. Yashima, Y. Okamoto, Angew Chem. Int. Ed. 37 (1998) 1922.
[102] K. Lorenz, E. Yashima, Y. Okamoto, Angew Chem. Int. Ed. 37 (1998) 2025.
[103] K. Rossen, J. Sager, Y. Sun, Chem Commun (1998) 115.
[104] S. Gebauer, S. Friebe, G. Scherer, G. Gübitz, G.-J. Krauss, J. Chromatogr. Sci. 36 (1998) 388.
[105] S. Borocci, M. Erba, G. Mancini, Langmuir 14 (1998) 1960.
[106] U. Schick, L. Jordi, S. Ricart, J. Veciana, K.H. Doetz, J.M. Moreto, J. Am. Chem. Soc. 120 (1998) 2283.
[107] T. Zimmermann, N. Pustet, A. Mannschreck, Monatshefte Chem. 130 (1999) 355.
[108] E. Rochlin, Z. Rappoport, F. Kastner, N. Pustet, A. Mannschreck, J. Org. Chem. 64 (1999) 8840.
[109] R. Kiesswetter, N. Pustet, F. Brandl, A. Mannschreck, Tetrahed. Asym. 10 (1999) 4677.

[110] T. Zimmermann, N. Pustet, A. Mannschreck, Monatshefte Chem. 130 (1999) 355.
[111] L. Loncar-Tomaskovic, K. Lorenz, A. Hergold-Brundic, D. Mrvos-Sermek, A. Nagl, M. Mintas, A. Mannschreck, Chirality 11 (1999) 363.
[112] J. Bella, S. Borocci, G. Mancini, Langmuir 15 (1999) 8025.
[113] A. Mandl, L. Nicoletti, M. Laemmerhofer, W. Lindner, J. Chromatogr. A 858 (1999) 1.
[114] J. Oxelbark, S. Allenmark, J. Org. Chem. 64 (1999) 1483.
[115] J. Oxelbark, S. Allenmark, J. Chem. Soc. Perkin. Trans. 2 (1999) 1587.
[116] T. Zimmermann, N. Pustet, A. Mannschreck, Monats. Chem. 131 (2000) 1083.
[117] G. Cannazza, D. Braghiroli, M. Baraldi, C. Parenti, J. Pharm. Biomed. 23 (2000) 117.
[118] F. Gasparrini, L. Lunazzi, A. Mazţanti, M. Pierini, K.M. Pietrosiwicz, C. Villani, J. Am. Chem. Soc. 122 (2000) 4776.
[119] M. Laemmerhofer, E. Tobler, W. Lindner, J. Chromatogr. A 887 (2000) 421.
[120] B.M. Ben-David, C. Yamamoto, Y. Okamoto, S.E. Biali, D. Kost, J. Org. Chem. 65 (2000) 8613.
[121] G. Bringmann, M. Heubes, M. Breuning, L. Goebel, M. Ochse, B. Schoener, O. Schupp, J. Org. Chem. 65 (2000) 722.
[122] O. Trapp, S. Caccamese, C. Schmidt, V. Bohmer, V. Schurig, Tetrahed. Asym. 12 (2001) 1395.
[123] A.C. Spivey, P. Charbonneau, T. Fekner, D.H. Hochmuth, A. Maddaford, C. Malardier-Jugroot, A.J. Redgrave, M.A. Whitehead, J. Org. Chem. 66 (2001) 7394.
[124] G. Cannazza, D. Braghiroli, A. Tait, M. Baraldi, C. Parenti, W. Lindner, Chirality 13 (2001) 94.
[125] G. Weseloh, C. Wolf, W.A. Koenig, Angew Chem. Int. Ed. 34 (1995) 1635.
[126] G. Weseloh, C. Wolf, W.A. König, Chirality 8 (1996) 441.
[127] A.S. Rathore, C. Horvath, Electrophoresis 18 (1997) 2935.
[128] K.P. Scharwaechter, D.H. Hochmuth, H. Dittmann, W.A. Koenig, Chirality 13 (2001) 679.
[129] G. Schoetz, O. Trapp, V. Schurig, Electrophoresis 22 (2001) 2409.
[130] G. Schoetz, O. Trapp, V. Schurig, Anal. Chem. 72 (2000) 2758.
[131] G. Schoetz, O. Trapp, V. Schurig, Enantiomer 5 (2000) 391.
[132] G. Schoetz, O. Trapp, V. Schurig, J. Cap. Electrophor. Microchip Techn. 6 (1999) 169.
[133] E. Tobler, M. Laemmerhofer, W. Lindner, J. Chromatogr. A 875 (2000) 341.
[134] E. Tobler, M. Laemmerhofer, G. Mancini, W. Lindner, Chirality 13 (2001) 641.
[135] O. Trapp, G. Schoetz, V. Schurig, Electrophoresis 22 (2001) 3185.
[136] E.L. Eliel, S.H. Wilen, Stereochemistry of Organic Compounds, Wiley, New York, 1994.
[137] O. Trapp, V. Schurig, J. High Resolut. Chromatogr. 23 (2000) 291.
[138] O. Trapp, V. Schurig, Comput. Chem 25 (2001) 187.
[139] O. Trapp, V. Schurig, J. Chromatogr. A 911 (2001) 167.
[140] W.J. Moore, in: Physical Chemistry, 4th ed., Prentice-Hall, Englewood Cliffs, NJ, 1972, Chapter 9.29.
[141] M. Jung, Program Simul, No. 620. Quantum Chemistry Program Exchange. QCPE Bull. 3 (1992) 12.
[142] R.A. Keller, J.C. Giddings, J. Chromatogr. 3 (1960) 205.
[143] R. Kramer, J. Chromatogr. 107 (1975) 241.
[144] E. Cremer, R. Kramer, J. Chromatogr. 107 (1975) 253.
[145] J. Hrouzek, J. Krupcík, M. Ceppan, S. Hatrík, P.A. Leclercq, Chem. Papers 54 (2001) 314.
[146] Microcal™ Origin™ Version 4.10, Microcal Software, One Roundhouse Plaza, Northampton, MA.
[147] Peak Fitting Module, Microcal Software, Northampton, MA, USA.
[148] N. Dyson, in: Chromatographic Integration Methods, Royal Society of Chemistry, The Science Park, Cambridge, 1990, Chapter 1.
[149] P. Oswald, J. Krupcik, K. Desmet, P. Sandra, D.W. Armstrong, in preparation.